Evaluating the Temperature Dependence of Heat-Transfer Based Detection: A Case Study with Caffeine and Molecularly Imprinted Polymers as Synthetic Receptors

K. Betlem[1], I. Mahmood[1], R. D. Seixas[2], I. Sadiki[3], R.L.D. Raimbault[3], C.W. Foster[1], R.D. Crapnell[1], S. Tedesco[1], C.E. Banks[1], J. Gruber[4], M. Peeters[1]*

1) Manchester Metropolitan University, Faculty of Science & Engineering, Div. of Chemistry & Environmental Science, John Dalton Building, Chester Street, M15GD, Manchester, United Kingdom.

2) Departamento de Engenharia Química, Escola Politécnica, Universidade de São Paulo, Avenida Prof. Luciano Gualberto, trav. 3, 380, CEP 05508-900 São Paulo, SP, Brazil.

3) IUT de Saint-Denis, Université Paris 13, Place du Mai 1945, 93206 Saint-Denis, France.

4) Departamento de Química Fundamental, Instituto de Química, Universidade de São Paulo, Av. Prof. Lineu Prestes, 748, CEP 05508-000 São Paulo, SP, Brazil.

Abstract:

Molecularly Imprinted Polymers (MIPs) are synthesized for the selective detection of caffeine. The polymerization process, monomer and crosslinker monomer composition are varied to determine the optimal synthesis procedure *via* batch rebinding experiments evaluated with optical detection. The selectivity is tested by comparing the response of caffeine to compounds with similar chemical structures (theophylline and theobromine) and dopamine, another neurotransmitter. Subsequently, the MIP polymer particles are integrated into bulk modified MIP screen-printed electrodes (MIP-modified SPEs). The sensors are used to measure caffeine content in various samples employing the Heat-Transfer Method (HTM), a low-cost and simple thermal detection method that is based on differences in thermal resistance at the solid-liquid interface. At first, the noise is minimized by adjusting the settings of temperature feedback loop. Second, the response of the MIP-modified SPE is studied at various temperatures ranging from 37 to 50 and 85 °C. The binding to MIP-modified SPEs has never been studied at elevated temperatures since most biomolecules are not stable at those temperatures.

Using caffeine as proof-of-concept, it is demonstrated that at 85 °C the detection limit is significantly enhanced due to higher signal to noise ratios and enhanced diffusion of the biomolecule. Thermal wave transport analysis (TWTA) is also optimized at 85 °C producing a limit of detection of ~1 nM. Next, MIP-modified SPEs are used to measure the caffeine concentration in complex samples including caffeinated beverages, spiked tap water and waste water samples.

The use of MIP-modified SPEs combined with thermal detection provides sensors that can be used for fast and low-cost detection performed *on-site,* which holds great potential for the determination of contaminants in environmental samples. The platform is generic and by adapting the MIP layer, we can expand to this a range of relevant targets.

Keywords: Molecularly Imprinted Polymers (MIPs), heat-transfer method (HTM), screen-printing technology, caffeine, environmental contamination.

Corresponding author: Dr. Marloes Peeters

Manchester Metropolitan University, Chester Street, M1 5GD

Manchester, United Kingdom.

Phone: + 44 – (0)161 – 247 1450

Fax: +44 (0)1612476318

E-mail: m.peeters@mmu.ac.uk

1. Introduction

Caffeine belongs to the class of methylxanthines and is a cardiac and cerebral stimulant [1, 2]. It is present in many pharmaceuticals because of certain analgesic effects in cough, cold and headache medicine [3]. In combination with its use in food and beverages, caffeine is considered the most widely consumed drug in the world [4]. It is also used as an anthropogenic marker for waste water contamination of surface waters and the presence of caffeine can be correlated to the abundance of various microbial contaminants [5]. Levels of caffeine in waste water range generally from 200-300 µg/L [6] but for countries such as Greece [7] and Taiwan [8] concentrations between 5,000-13,000 ng/L were reported. Caffeine has also been ubiquitously found in surface water; in Swiss lakes and rivers

concentrations of ~2ng/L were reported [5] and a comprehensive study performed in Brazil found 93% of all surface water samples contained caffeine [9]. Contamination of surface water with micropollutants is a serious concern since this is used to produce drinking water in water treatment plants [10].

For a number of micropollutants, environmental quality standards have been set by the European Parliament [11]. In 2016, Swiss legislation set new effluent standards and required companies to incorporate novel treatment processes such as the addition of powdered activated carbon units followed by sand filtration [12]. This technique has been able to remove over 80 % of micropollutants. The presence of these compounds in municipal water also has a significant effect on aquatic life since caffeine has been suspected to decrease hemocyte adherence in mussels [13]. Fresh water mussels exposed to a number of micropollutants showed signs of inflammatory responses related to stress and caffeine potentially affects their reproduction [14, 15].

Therefore, there is a great need for the sensitive detection of caffeine as a contaminant in drug samples, waste water and surface water. Traditional detection of caffeine include chromatographic techniques such as High-Performance Liquid Chromatography-Mass Spectrometry (HPLC-MS) [16, 17], electrospray triple-quadrupole mass spectrometry (LC-MS/MS) [9], Gas Chromatograph Mass Spectrometry (GC-MS) [18, 19], micro gravimetric methods [20] or the use of immunoassays [21, 22]. All those techniques are either time-consuming or require the use of a lab environment, which does not allow the measurement of water quality on-site with a portable device [23]. Few optical sensors have been reported in literature, which would offer fast (<1 min) detection of increased caffeine levels in beverages [24, 25]. While these sensor platforms are easy to use, they are not label-free and exhibit low sensitivity.

In this manuscript, we will explore the use of Molecularly Imprinted Polymers (MIPs) combined with thermal read-out for the low-cost, fast and selective determination of caffeine in a range of buffered solutions and complex food samples. To test the selectivity of this sensing platform, the response of caffeine will be compared to dopamine, another stimulant of the central nervous system, as well as chemically similar compounds theophylline and theobromine, for which MIP based sensors have been reported [26, 27].

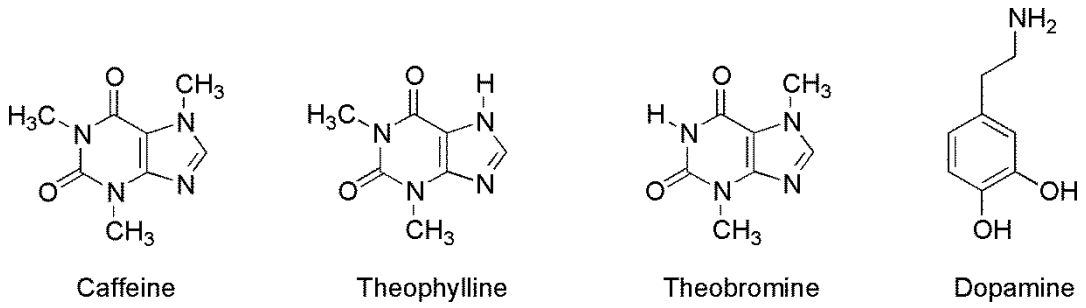

Figure 1: *Chemical structures of theobromine, caffeine, theophylline and dopamine.*

MIPs are porous materials that contain high-affinity nanocavities for their template molecules [28-30]. Contrary to antibodies, they possess superior thermal and chemical stability, are low-cost, and can be manufactured in bulk quantities [31, 32]. Several MIPs for caffeine have been developed for the extraction and purification of samples [33, 34]. MIP-based caffeine sensors are mainly based on electrochemical detection [35-37] or gravimetric methods [38]. The use of the Heat-Transfer Method (HTM) for detection offers advantages of fast, low-cost and straightforward analysis [39]. This thermal method relies on monitoring the thermal resistance at the solid-liquid interface and has found numerous applications in the field of DNA mutations [40], biomolecule detection [41] and phase transitions in lipids [42]. This work will build upon a recent study where MIP particles were mixed with screen-printing ink [43] in order to manufacture mass-producible MIP-modified SPEs (Screen-Printed Electrodes). These MIP-modified SPEs are used to determine neurotransmitter concentrations, which meant due to the instability of the molecules thermal analysis was limited to a temperature range up to 40.0 °C. Caffeine is thermally stable up to ~180 °C [44] and therefore the ideal candidate to evaluate the influence of temperature on detection with HTM. With these results, we will demonstrate that higher temperatures, up to 85 °C, minimize noise on the signal and enhance the signal-to-noise ratio, thereby significantly increasing the limit of detection. It is possible to use these MIP-modified SPEs for the thermal detection with a range of food samples, which is a proof-of-concept for a portable sensor that can determine samples contaminated with caffeine. In the future, this could be extended to a sensitive platform for determination of water quality in areas with limited infrastructures. By adapting the MIP layer, it will be possible to simultaneously measure caffeine and other pharmaceutical or microbial compounds.

2. Experimental

2.1 Reagents

Trimethylolpropane trimethacrylate (TRIM), methacrylic acid (MAA), dopamine hydrochloride salt (99 %), (hydroxyethyl)methacrylate (HEMA), and dimethylsulfoxide (DMSO) were purchased from Acros (Loughborough, United Kingdom). Prior to polymerization, the stabilizers in the MAA, HEMA and TRIM were removed by passing the solutions over a column packed with alumina. Acrylamide (AA), phosphate buffered saline tablets (PBS), 4,4'-azobis(4-cyanovaleric acid), dimethyl sulfoxide-d_6, theophylline, theobromine and caffeine were purchased from Sigma Aldrich (Gillingham, United Kingdom).

2.2 MIP and NIP syntheses

MIPs for caffeine were synthesized with varying compositions, which are listed in Table 1. The general functionalization procedure includes mixing of the template caffeine (0.35 mmol) with the monomer (1.3 or 2.6 mmol) in 7.0 mL of DMSO. Subsequently, the crosslinker monomer TRIM (3.0 mmol) was added followed by the initiator 4,4-azobis(4-cyanovaleric acid) (50 mg). The mixture was sonicated for 5 min and degassed with N_2 prior to the start of polymerization. Polymerization was initiated by heating up the sample up to 65 °C and maintaining the mixture at this temperature for 12 h, ensuring polymerisation reached completion. The obtained bulk powder was ground to obtain a fine powder and particles were sieved to obtain only those with particles size of less than 50 μm. Caffeine was removed by continuous Soxhlet extraction with a mixture of methanol and water (50/50) and a mixture of acetic acid and methanol (50/50) until UV no longer detects traces of caffeine in the filtrate. The powders were washed with water and dried overnight under vacuum. NIPs were synthesized in the same manner but without the addition of the template.

Table 1. The composition of the different MIPs, listing the amount of template, functional monomer, crosslinker monomers, initiator, and porogen used.

	MIP-1	**MIP-2**	**MIP-3**	**MIP-4**	**MIP-5**
Caffeine (mmol)	0.35	0.35	0.35	0.35	0.35
MAA (mmol)	1.3	2.6	-	-	0.7
Acrylamide (mmol)	-	-	1.3	-	-
HEMA (mmol)	-	-	-	1.3	0.7
TRIM (mmol)	3.0	3.0	3.0	3.0	3.0
Initiator (mg)	50	50	50	50	30
DMSO (mL)	7.0	7.0	7.0	7.0	4.0

2.3 Batch rebinding experiments evaluated with optical detection

Batch rebinding experiments were performed and optical detection was used to evaluate the binding of caffeine to the MIP and NIP powders. The caffeine concentration was determined by measuring the absorbance at λ=281 nm with an Agilent 8453 spectrophotometer (Stockport, United Kingdom). In each experiment, 10 mg of MIP or NIP powder was added to 5.0 mL of PBS solutions with caffeine concentrations between 0 – 0.3 mM. The resulting suspensions were placed on a rocking table (110 rpm) for time intervals ranging from 15 min to 15 h, with the maximum binding occurring at 1 h. The samples were then filtered and the free concentration of caffeine (C_f) in the filtrate was determined by UV-vis spectroscopy. The imprint factor (IF) was used as a measure of specificity of the MIPs and were calculated with the constructed binding isotherms.

2.4 HTM and TWTA measurements with MIP-modified SPEs

The procedure to prepare the MIP-modified SPEs is described in detail in ref [43]. Briefly, MIP1 and NIP1 were incorporated into the bulk ink of the SPEs with a mass percentage of 30 % of mass particulate *vs*. mass ink. A carbon-graphite ink formulation (Product Code: C2000802P2; Gwent Electronic

Materials Ltd, UK) was printed onto a standard polyester substrate and cured at 60 °C for 30 min. These MIP-modified SPEs were used in all described HTM and TWTA measurements.

All thermal measurements were performed with a 3D printed flow cell with an inner volume of 110 µL that was designed in house [45]. This flow cell was sealed off with an O-ring and connected to the HTM set up that is described in [40]. MIP-modified SPEs are pressed onto a copper block, which serves as a heat sink, and which temperature T_1 is actively steered with a Proportional-Integral-Derivative (PID) controller. The temperature in the liquid (T_2) is measured every second with a type K thermocouple at 1.7 mm above the chip surface. This allows for the determination of the thermal resistance at the solid-liquid interface, which is defined as the temperature gradient ($T_1 – T_2$) divided by the power provided to the heat source.

The PID parameters affect the stability of the power signal, hence they have an impact upon the noise and thereby the sensitivity of the developed sensor platform. The optimal settings depend on the flow cell, electrode, temperature, and buffer composition. Previous research [46] with MIP-modified SPEs developed for noradrenaline demonstrated the optimal PID settings in buffered solution were 1,10,0 at T=37 °C. In this contribution, initial screening of the parameters was performed at 30 °C by measuring the thermal resistance when MIP electrodes were exposed to a PBS buffer (pH = 7.4) solution for 1 h. P was varied from 1-8, I from 1-8 and D 0-0.5. Four settings, respectively, PID 1,8,0, 1,8,0.1, 1,7,0, and 1,7,0.1, resulted in the lowest percentage errors over the signal and were further examined at temperatures of 50, 70 and 90 °C. Both caffeine and the MIPs were stable at these elevated temperatures, which was confirmed by thermogravimetric analysis (TGA) performed with a TG4000 from Perkin Elmer (London, United Kingdom). This information is enclosed in **Appendix A.**

In further measurements, the configuration of the PID parameters was fixed at 1,8,0. Subsequently, the influence of temperature on the binding of the template to the polymer layer was determined by measuring MIP-modified SPEs at 37, 50 and 85 °C. The MIP-modified SPE were first stabilized for 45 min PBS and then solutions of increasing caffeine concentrations (2.5, 5, 10, 25, 50, 100, and 250 nM) in PBS were added into the flow cell with an automated NE500 programmable syringe pump from ProSense (Oosterhout, the Netherlands). The solutions were injected at intervals of 30 min with a flow rate of 250 µL/min. The thermal resistance (R_{th}) was monitored over time and determined at each

concentration. This was used to construct dose-response curves, where the limit of detection was calculated using the three sigma method in the linear range of the sensor. To establish the specificity of the sensor platform, identical measurements were performed with a NIP-modified SPE. The selectivity was evaluated by exposing the sensor to a solution with a high (1 mM) concentration of similar molecules, including theophylline, theobromine and neurotransmitter dopamine.

Next, the performance of the MIP-based sensors were evaluated using a beverage known to contain caffeine. Both coffee (Aldi's Fairtrade Colombian Instant Coffee, UK – 2 % caffeine content) and black tea (Tesco original, Cheshunt, UK – 0.7 % tea content according to label) were measured in the HTM set up. For the coffee sample, 2.6 mg of instant coffee was dissolved in 10 mL of warm PBS. The maximum caffeine content is estimated to be 2 %, which was used to make dilutions containing approximately 1 and 37 μM of caffeine in PBS. The tea samples were made by serial dilutions of 1/100 and 1/10 dilution in PBS before being measured.

Finally, the performance of the MIP-modified SPEs was evaluated by measuring spiked tap water and wastewater samples (0 – 100 nM). The selectivity was evaluated by determining caffeine concentrations in PBS samples that were in the presence of an excess of theophylline (250 nM). The wastewaters samples utilised were kindly provided by Viridor (ltd.) Recycling Centre, Greater Manchester, UK. These are constituted by the digested organic fraction of Municipal Solid Waste (MSW) treated at the plant, using a thermophilic anaerobic digestion process (55 °C) for biogas production. The MSW wastewater samples were collected from the primary bioreactor at the end of their hydraulic retention time. The liquid fraction of digested wastewaters needs to be analysed for land spreading applications for use as biofertiliser or to be released in the environment. Therefore, the determination of contaminants, especially from MSW substrates, is crucial to establish the digestate's upgrading requirements and its environmental impact. To prevent sedimentation from blocking the tubing and fouling the electrode, the sample (25 mL) was centrifuged at 4200 rpm for 1 h, the supernatant was then collected and used for all further HTM measurements. The tap water was used without any additional pre-treatment and stored at room temperature (~20 °C).

In addition to the standard HTM measurements thermal wave transport analysis (TWTA) measurements were performed as described by Peeters *et al*. [43]. In short, the MIP-modified SPE was exposed to a

thermal wave (amplitude of 0.1 °C, frequency range from 0.0083 to 0.05 Hz) originating from the heat-sink, where T_2 recorded the response of this thermal wave in the liquid. The delay in the response time is caused at the solid-liquid interface and the binding of caffeine in the MIP layer. By comparing the delay in response time of different caffeine concentrations to a pure aqueous solution one is able to solely study the binding effect. A conversion of this delay to a phase shift was performed by taking the time of one thermal wave (pure aqueous solution, c=0 of caffeine concentration) measured at the output as 360 °. Finally, by plotting the normalized phase shift versus the caffeine concentrations a dose-response curve was obtained.

2.5 Evaluation of monomer-template binding using NMR analysis

NMR analysis was performed according to Xu *et al*. [24], with some minor changes to accommodate the current study. MAA (1.6 mg) was dissolved in 1.0 mL of either DMSO-D_6 or $CDCl_3$, resulting in a 18.4 mM concentration. NMR spectra were obtained using a Jeol ECS-400 spectrometer (Welwyn Garden City, UK). Hereafter, the concentration of caffeine in the solution was increased by adding solutions to vials containing 0.9, 1.8, 3.6, 7.2 or 14.4 mg of caffeine. After every addition of caffeine, the solution was transferred back to the original NMR tube and a new ^1H spectrum was recorded.

To determine if the obtained peak shifts are concentration dependent or caused by an interaction between monomer and template, a set of control spectra was obtained for both pure caffeine and pure MAA in DMSO-D_6. Therefore, three NMR tubes were prepared containing either a low, medium or high concentration of target molecule or monomer. For the caffeine tubes this resulted in concentrations of 4.6, 36.8 and 147.2 mM and for MAA, the concentrations were 0.2, 1.3 and 10.4 mM.

All recorded data were further processed using MestreNova (v6.0.2-5475).

3. Results

3.1 Batch rebinding results

First, batch rebinding experiments with MIP1-4 were performed that have a similar composition but differ in the functional monomer that was used. The time of the experiments was fixed at 1 h since after

this time no increase in the binding to the MIP particles was observed. In each experiment, 5 mL of caffeine solutions in PBS (C_i = 0-0.5 mM) were added to 20 mg of the MIP particles. In Table 2, the amount of template bound per gram to MIPs and NIPs were compared at a free concentration of C_f = 0.22 mM. The amount bound at C_f was determined with a two-parameter allometric fit.

Table 2. The amount of binding for each MIP and NIP at C_f = 0.22 mM.

Polymers	S_b [µmol/g]	Impact factor C_f = 0.22 mM
MIP1	19.5	3.5
NIP1	5.6	
MIP2	14.3	1.5
NIP2	9.6	
MIP3	34.6	4.1
NIP3	8.5	
MIP4	42.2	2.8
NIP4	15.0	
MIP5	6.2	2.9
NIP5	17.8	

The difference between MIP1 and MIP2 is the amount of monomer used, 4x *vs* 8x. Table 1 shows that increasing the amount of monomer had an adverse effect on binding and increased the amount of non-specific binding due to increasing the number of charges on the polymer surface. MIP3 and MIP4 showed a significantly higher amount of binding at elevated concentrations, with the IF of MIP3 being significantly higher due to less non-specific binding. MIP5 is a combination of two different monomers and balances of charges, which showed specific binding towards caffeine but its IF values were lower compared to some other MIPs. Therefore, MIP1 and MIP3 were further examined for their selectivity

towards caffeine by comparing the binding to that of similar molecules theophylline and theobromine. The results for MIP3 are listed in Figure 2.

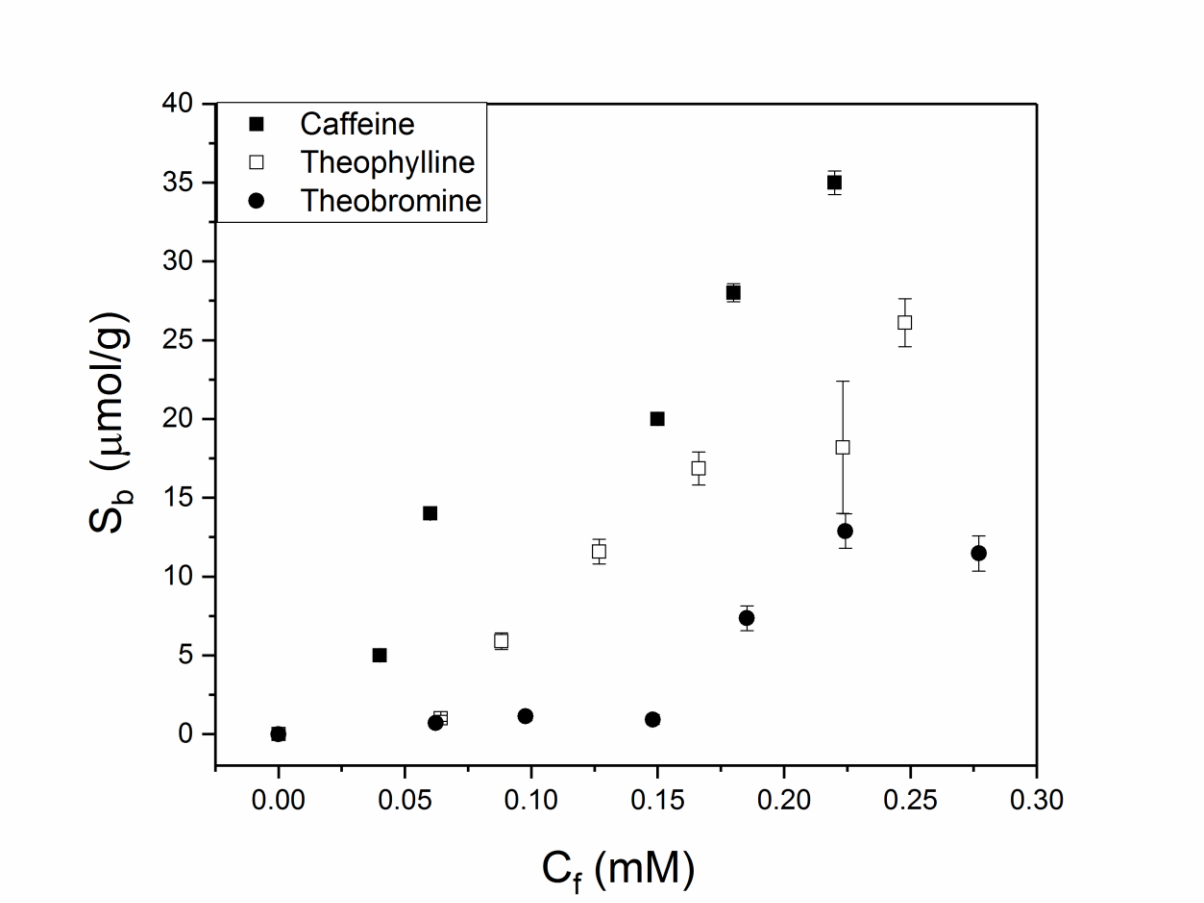

Figure 2. Binding isotherms of MIP3 upon exposure to caffeine (solid squares), theophylline (open squares) and theobromine (solid circles) solutions in PBS. Error bars were calculated by averaging out the results of three independent measurements.

As can be seen in Figure 2, MIP3 absorbs ~34 µmol/g caffeine at C_f = 0.22 mM. This is significantly higher than for instance theobromine, absorbing only ~12 µmol/g, which differs only by one methyl group compared to chemical structure of caffeine. The binding of theophylline is considerably higher than theobromine but still lower than for caffeine. At low concentrations the differences are in order of factor of three (at C_f = 0.05 mM, considering fit data, ~10 µmol/g for caffeine and ~3 µmol/g for theophylline) but at higher concentrations smaller differences are observed due to gradual occupation of the binding sites. The relevant concentration range of caffeine in relevant water samples is in the low

nanomolar range. Therefore, it was decided to evaluate the performance of the sensor to discriminate caffeine from its competitor molecule in the nanomolar concentration, for which it is required to use a more sensitive read-out strategy such as HTM.

3.2 Thermal resistance measurements MIP-modified SPEs in phosphate buffered saline solutions

In previous MIP-modified SPE measurements, the temperature of the heat sink was kept constant at 37 °C to mimic body temperature. In this work, it was first evaluated whether it was possible to measure at a lower temperature since this could be beneficial for performing measurements on-site.

Therefore, MIP-modified SPEs printed onto polyester substrates were mounted in the thermal set up and the thermal resistance was measured for electrodes exposed to PBS solution for 1 h. MIP1 was incorporated into the SPEs despite MIP3 having a slightly higher IF value. The reason for this is two-fold: first, mixing of MIP3 within the graphitic ink was less successful compared to MIP1, and, second, acrylamide is a soft material and this interferes with the stability of the sensors and adherence to the substrate. MIP5 was also incorporated into SPEs but demonstrated a lower thermal resistance compared to MIP1.

The temperature of the heat sink (T_1) was set at 30 °C and the PID parameters were varied. Table 3 shows the optimal settings, P (1), I (7, 8) and D (0, 0.1), where the percentage errors over the signal was determined by averaging 600 data points. The error on the signal for all configurations was ~2 %, which is at least a factor of two higher compared to optimized data previously reported [46] for the MIP-modified SPEs designed for noradrenaline that were measured at 37 °C. Therefore, measurements at lower temperature were not deemed suitable for the detection of caffeine. Subsequently, the influence of the temperature on the noise levels was further examined by measuring the same PID settings at 50, 70 and 90 °C.

Table 3. MIP-modified SPEs were exposed to PBS for 1 h and the effect of the temperature and PID settings on noise levels on the signal was evaluated. Standard deviation (SD) was determined by averaging out R_{th} values of at least 600 measurement points.

P	I	D	T	R_{th}	SD	Percentage error
			°C	°C/W	°C/W	%
1	8	0.0	30	6.97	0.14	2.00
1	8	0.0	50	5.79	0.04	1.00
1	8	0.0	70	5.47	0.02	0.40
1	8	0.0	90	4.71	0.05	1.00
1	8	0.1	30	7.31	0.13	2.00
1	8	0.1	50	5.91	0.04	1.00
1	8	0.1	70	5.40	0.02	0.40
1	8	0.1	90	4.79	0.02	0.40
1	7	0.0	30	6.91	0.14	2.09
1	7	0.0	50	5.08	0.03	0.68
1	7	0.0	70	4.58	0.02	0.45
1	7	0.0	90	4.55	0.04	0.95
1	7	0.1	30	6.93	0.15	2.15
1	7	0.1	50	5.33	0.04	0.72
1	7	0.1	70	4.81	0.02	0.47
1	7	0.1	90	4.74	0.03	0.56

Table 3 demonstrates that increasing the temperature to 50 °C lowers the noise two-fold compared to temperatures of 30 °C. This was expected for such a feedback loop since it is easier to control larger differences in temperature compared to minimal oscillations. The lowest value (0.72 %) was attained with PID 1,7,0.1, which was lower than the previously reported MIP-modified SPEs values. By

increasing the temperature further to 70 °C, the noise was further reduced down to ~0.4 %. Temperatures of 90 °C did not lead to further reductions in noise, which could be because this is close to the boiling point of PBS leading to fluctuations in the liquid. The measurements were repeated at 85 °C with both a MIP and NIP-SPE, leading to noise levels of around ~0.3 %, indicating this is the optimal measurement temperature and optimal PID settings. Therefore, in all further measurements the PID parameters were fixed at 1,8,0.

First, to establish a reference, the response in thermal resistance for NIP-modified SPEs (T = 85 °C) was measured after they were exposed to PBS solutions with varying caffeine concentrations (0-250 nM). The thermal resistance increased after the addition of solutions at room temperature but quickly stabilized back to the baseline level (**Appendix B**) indicating no specific binding to the NIP layer. Subsequently, the thermal resistance of the MIP-modified SPEs was measured after exposing them to identical PBS solutions with caffeine concentrations to construct dose-response curves. Contrary to the NIP, clear increases in the resistance were documented as are shown in Figure 3. This is the first report in literature of MIP measurements with HTM performed at elevated temperatures (50 and 85 °C). These results were compared to the standard temperature of 37 °C. The absolute R_{th} values are shown in Figure 3A, while Figure 3B represents the percentage increase in R_{th} at given concentrations with the error calculated from the standard deviation of 600 data points.

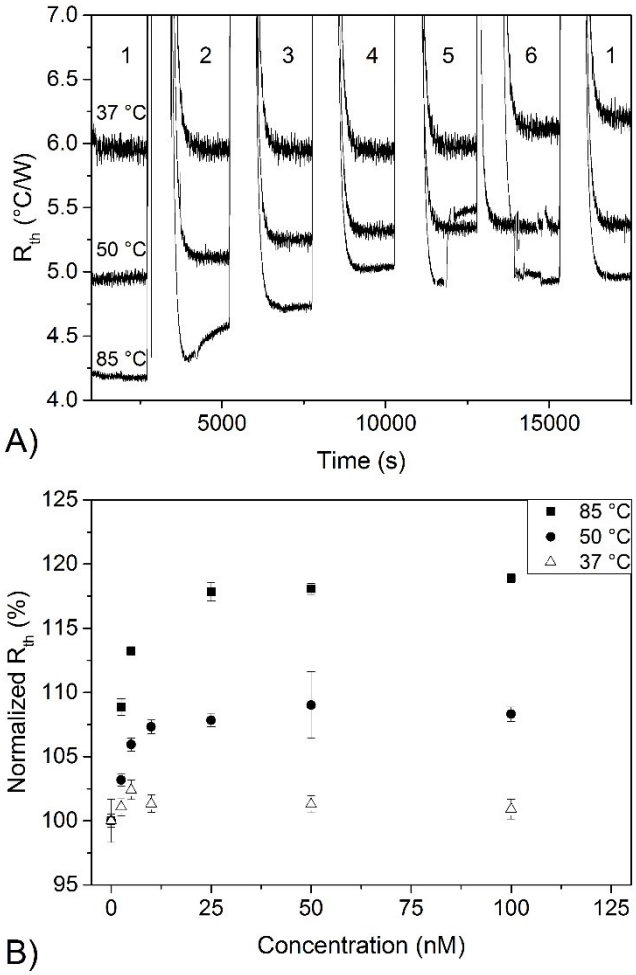

Figure 3. A) demonstrates the thermal resistance in time at T = 37, 50 and 85 °C when the MIP-modified SPEs were exposed to buffered caffeine solutions with increasing concentrations. The numbers correspond to additions of a pure PBS solution (1), and increasing concentration of caffeine (0, 2.5, 5, 10, 25, 50, 100 nM) indicated by numbers 2-6. B) shows the HTM dose-response curves for the MIP, where the percental increase was calculated by dividing the R_{th} at a certain concentration by the baseline level.

At higher temperatures, the difference between the set temperature (T_1) and the measured temperature in the liquid (T_2) was lower and this resulted in a lower thermal resistance. The baseline at 37 °C was 5.8 ± 0.05 °C/W, which was lowered to 4.95 ± 0.03 °C/W, and further reduced to 4.17 ± 0.02 °C/W at 85 °C. These results also demonstrated that the noise on the signal depends on the temperature, which

was in line with what previously was observed when varying the PID parameters. The sensitivity was also significantly different; at 37 °C no changes were observed until 50 nM, an increase was seen at 5 nM at 50 °C, while for 85 °C this was the case at 2.5 nM. The effective size at 100 nM varied between 1 % (37 °C), 8 % (50 °C) and 19 % (85 °C). Limits of detection were determined according to the three sigma method and varied from ~40 nM (37 °C) to ~10 nM (50 °C) and <1 nM (85 °C). This means it is possible to fine-tune the limit of detection (LOD) by changing the temperature; while at 85 °C it would enable trace detection in drinking water and at 37 °C there is potential to determine caffeine levels in food samples that are present in significantly higher quantities. The results obtained in this study compare favourably to other methods reported in literature, a sample of which are shown in Table 4.

Table 4. A table showing various detection methods for caffeine found in literature along with the detection limits obtained in each study.

Method	Recognition Element	Electrode Material	Sample	LoD/ $x10^{-8}$ M	LoQ/ $x10^{-8}$ M	Reference
DPV	Bismuth film	SPE	Beverages/Coffee	2.7	9.0	[47]
DPASV	Graphene/nafion	SPE	Beverages/Coffee	2.1	6.6	[48]
DPV	MIP	Carbon paste	Beverages/Tea	1.5	-	[49]
SLM-PZ	MIP	Au	Coffee/Tea	2.8	-	[50]
Thermal	MIP	SPE	Coffee/Tea	0.1	-	This Work

Abbreviations: DPV (Differential Pulse Voltammetry), DPASV (Differential Pulse Anodic Stripping Voltammetry), SLM-PZ (supported liquid-membrane piezoelectric), SPE (Screen Printed Electrode).

The re-usability of the sensor set up was also evaluated and is enclosed in **Appendix C.** It demonstrates that washing with PBS is not sufficient to regenerate the sensor platform at high concentrations and the caffeine binds to the MIP layer with high affinity. A better alternative would be to flush with ethanol at a low flow rate but previous experiments demonstrated that resulted in cracks in the polymer-based flow cell. SPEs are low-cost (£0.10 or less for electrodes printed in-house) and therefore, it would be more expensive to regenerate the sensor platform than to use a freshly prepared electrode. In most

environmental applications there are low traces of caffeine present, meaning regeneration with PBS at high flow rates could potentially be considered for regeneration of the electrodes.

The next step is to evaluate the selectivity at 85 °C, which was carried out by exposing the MIP-modified SPEs to 1 mM solutions of compounds that possess a similarity in chemical structure or biological function. The results are represented in Figure 4. In addition, caffeine concentrations were determined in the presence of an excess of theophylline. These results, presented in **Appendix D,** indicate that detection is significantly impacted by the presence of a competitor molecule.

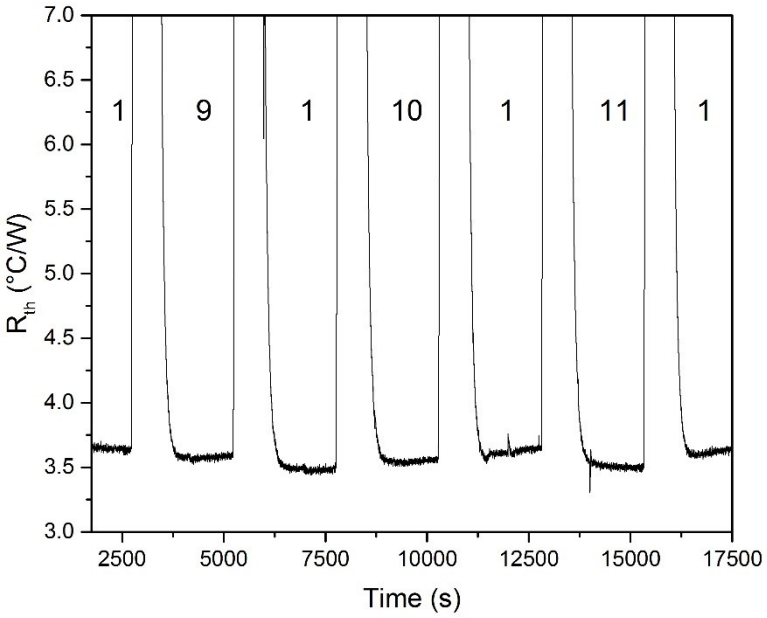

Figure 4. demonstrates the thermal resistance at 85 °C in time when the MIP-modified SPEs were stabilized in PBS (1), followed by addition of 1 mM in PBS solutions of theophylline (9), dopamine (10) and theobromine (11). Between each addition, a washing step with PBS (1) was performed to remove molecules in solution or loosely bound to the MIP-modified SPE surface.

The electrode was first stabilized in PBS, which led to a stable baseline signal of 3.62 ± 0.03 °C/W. The addition of a solution with a high theophylline concentration (1 mM in PBS) did not result in a significant difference in thermal resistance, whereas with caffeine solutions with a low concentration (5 nM or higher) gave a significant thermal response. The electrodes were washed with PBS in between

the steps. Additions of solutions of a high concentration of either the neurotransmitter dopamine or theobromine, which only differs by one methyl group compared to caffeine, did not have a significant impact on the thermal resistance. These results were in line with the conducted batch rebinding experiments that were analysed with optical detection, demonstrating the high selectivity of the developed MIP-based sensor platforms.

The next step was to evaluate the performance of the MIP-based sensors in complex matrices, including coffee and tea samples. Therefore, MIP-modified SPEs were first stabilized in PBS after which dilutions of instant coffee in PBS were added. The results at 50 and 85 °C are shown in Figure 5. There was no significant response at 37 °C and therefore these results were omitted from the graph.

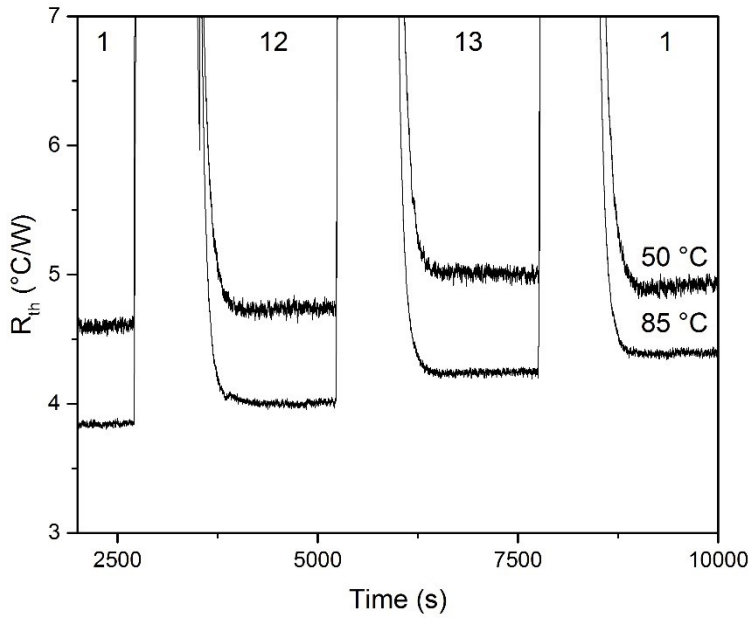

Figure 5. The thermal resistance in time is represented after stabilization in PBS (1) followed by additions of instant coffee samples diluted in PBS (12, 13). The caffeine content of 12 is estimated at 1 μM whereas the content of 13 was estimated at 37 μM. The measurements were performed at 50 °C (top) and 85 °C (bottom).

The coffee matrix was prepared from instant coffee with a predetermined caffeine content of 2 % according to the manufacturer's label. After subsequent exposure of caffeine-enriched PBS solutions, a clear difference in the thermal resistance was observed that were dependent on the measurement

temperature that was employed. The MIP-modified SPEs stabilized at 4.6 °C/W in PBS (T = 50 °C), with an increase to ~5.0 °C/W (8.7 % increase) in a matrix of PBS and coffee containing approximately 37 µM of caffeine. The percentage increase at 85 °C was equal to ~21 %, which was similar to the percentage increase measured at the highest concentration that could be determined in a buffered solution (100 nM). Quantification of caffeine levels above that range is complicated due to saturation of the electrodes and measuring outside of the linear range of the sensor platform. However, it was a first proof-of-concept of measuring complicated samples such as beverages.

To take this a step further, we examined tea samples that were diluted in PBS (1/100 and 1/10) since their caffeine content is significantly lower compared to instant coffee (2 % *vs*. 0.7 %). These experiments were performed at both 37 and 85 °C to highlight the effect of measurement temperature. Experiments were performed in duplicate, with minimal variation (0.5 %) in the signal.

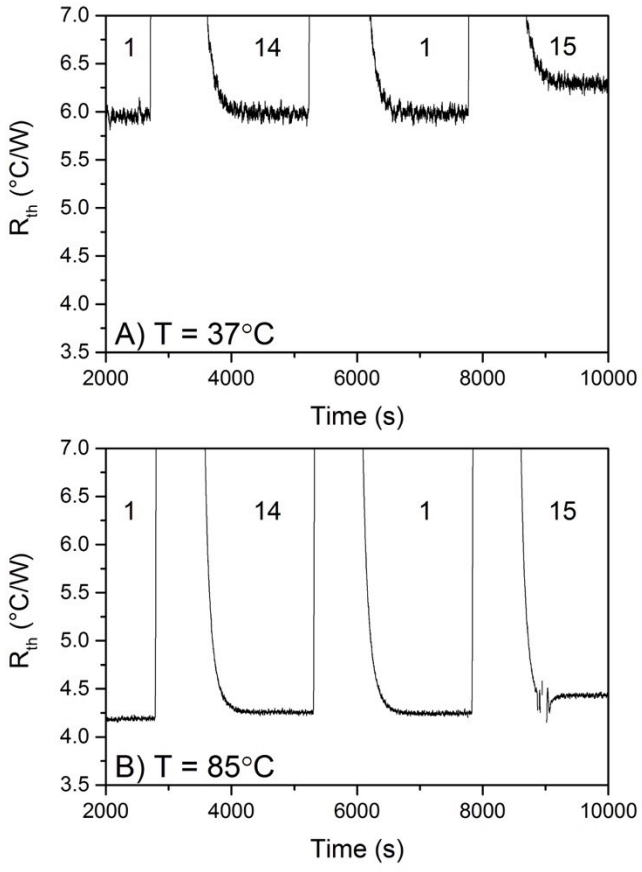

Figure 6. MIP-modified SPEs were stabilized in PBS (1), followed by the addition of (14) diluted tea (1/100) in PBS solution, washing with PBS (1) and subsequent addition of (15) a more concentrated tea (1/10 in PBS) solution. A) shows the response at 37 °C while B) provides data for 85 °C.

The thermal resistance stabilized at 6.0 ± 0.1 °C/W at 37 °C. The addition of diluted sample of tea, 1/100 tea *vs*. PBS, did not lead to a significant change in the thermal signal. However, an increase in the thermal resistance of 4.2 % to 6.2 ± 0.1 °C/W was measured for the addition of 1/10 tea *vs*. PBS. This procedure was repeated at 85 °C since the sensitivity in buffered solutions was distinctly higher than for measurements performed at body temperature.

The thermal resistance stabilized at 4.20 ± 0.02 °C/W at 85 °C, which is in line with previous results (Figure 3). Addition of a 1/100 tea sample diluted with PBS led to a minor but significant increase to 4.25 ± 0.02 °C/W. This corresponds to a 1 % increase in the signal, which according to the dose-response curve at this temperature is equal to a caffeine concentration of ~1 nM. A further increase in the thermal resistance of 6.7 % was measured for 1/10 dilution of tea at 4.46 ± 0.02 °C/W. However, it has to be considered that these dose-curves were constructed in buffered solutions and the presence of other molecules within the tea sample can affect the binding.

To further examine the effect of the matrix on the detection of caffeine, spiked tap water and wastewater samples (0-100 nM) were evaluated at a temperature of 85°C. These results for the MIP and NIP sensor are presented in Figure 7, where Figure 7a depicts the evolution of the thermal resistance in time and Figure 7b provides the corresponding dose-response curves.

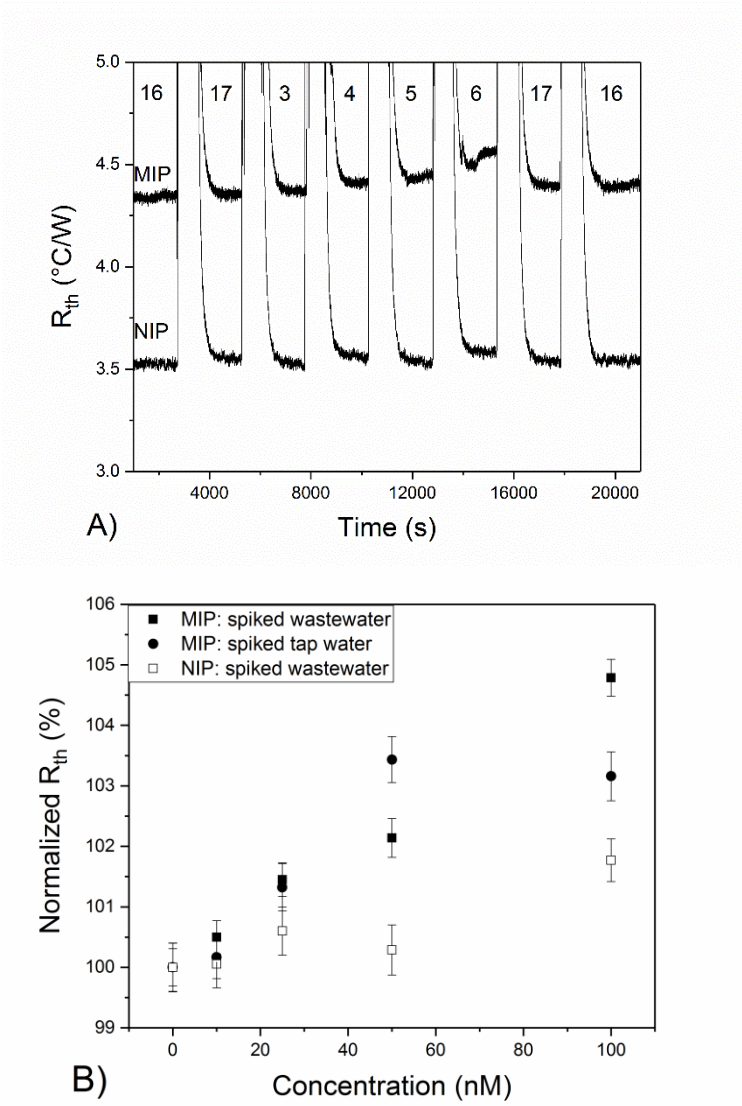

Figure 7A) MIP-modified SPEs and NIP-modified SPEs were stabilized in Miliq water before being changed to wastewater, followed by the addition of wastewater samples spiked with caffeine and subsequently flushing with wastewater and Miliq. The response was measured at 85°C and A) represents the thermal resistance over time. B) demonstrates the corresponding dose-response curves for MIP (filled squares) and NIP (open squares) measured in spiked wastewater samples, and the solid circles indicate the same measurement performed in spiked tap water samples. The error bars represent the normalized standard deviation on at least 180 data points.

The thermal resistance stabilized at 4.3 ± 0.1 °C/W at 85 °C for the MIP-modified SPE and 3.5 ± 0.1 °C/W for the NIP-SPE. This demonstrates that noise on the signal (0.1°C/W) was increased by a factor of three compared to measuring buffered samples (0.03°C/W), highlighting the influence of the matrix

on the electrodes. Upon addition of solutions spiked with 25 nM caffeine or more, significant increases in the thermal resistance were observed for the MIP-modified SPE. Spiking with 100 nM led to changes of ~5% in wastewater and 3% in tap water for the MIP electrodes, with an increase of ~2% for the NIP electrodes. The increase observed for the NIP-modified electrode can most likely be attributed due to fouling of the electrodes with contaminants in water; for instance, microorganisms can adhere to the surface. For sensing purposes, it would therefore be recommended to measure MIP simultaneously with the NIP to establish an appropriate reference. While the sensor performance is lower compared to the response in buffered solutions, we can still measure within the low nanomolar regime and this is a first demonstration of proof-of-application for these sensor platforms. It has to be noted minimal or no sample pre-treatment was performed on these samples, and noise on the signal and level of detection can be boosted by adjusting this procedure.

3.3 Thermal Wave Transport Analysis (TWTA) results

In previous work, it was shown that TWTA is a novel thermal technique benefiting from a short measurement time [43, 46]. A thermal wave with an amplitude of 0.1 °C was applied around the set point of 85 °C, where this was limited to 37 °C in previous measurements with MIP-based sensor platforms. With this increase in baseline temperature, it was required to determine the optimum input frequency of the thermal wave. Therefore, the input frequency was altered between 0.0083 Hz and 0.05 Hz and applied for 17 minutes before the injection of a different concentration of caffeine. The time delay between input and registration in the liquid for every input frequency and concentration is represented in Figure 8. From Figure 8A, it becomes clear that a frequency of 0.017 Hz shows the best response when performing measurements at 85 °C. The time delay of the 0.017 Hz input frequency was subsequently converted to a phase shift. By normalizing the phase shift to the baseline, the dose-response curve in Figure 8B was constructed. The linear range for the sensor on the dose-response is between 0 and 25 nM, after which saturation of the signal was observed. The LOD for the region of linear fit was estimated to be ~1 nM.

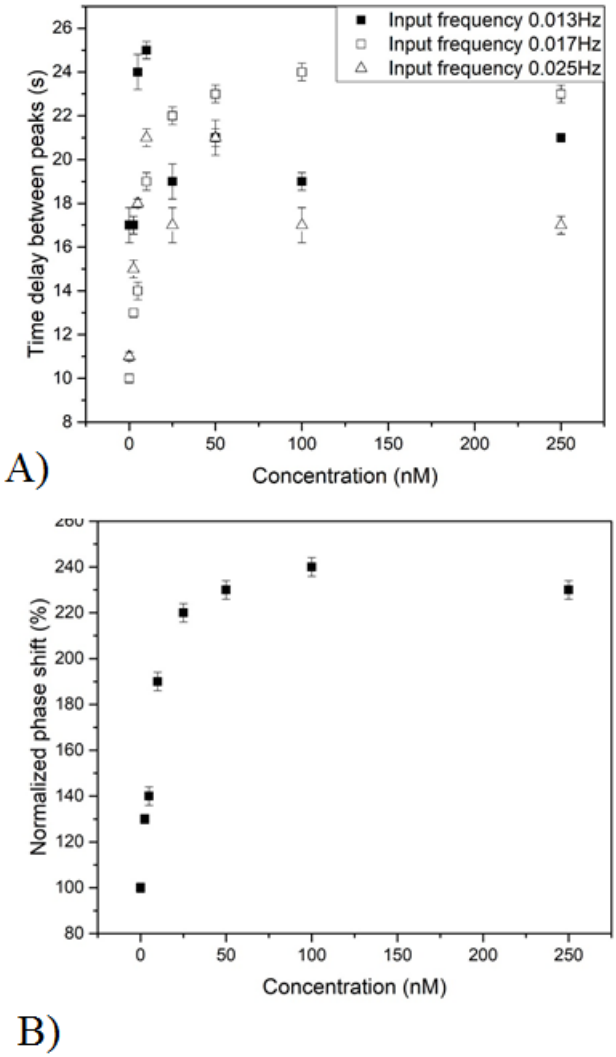

Figure 8. A) TWTA of the input frequencies 0.013 (solid squares), 0.017 (open squares) and 0.025 Hz (open triangles), measured at T = 85 °C. The thermal wave was applied on a range of caffeine concentrations (0, 2.5, 5, 10, 25, 50, 100 and 250 nM). B) Normalized TWTA dose-response for caffeine that was determined at the optimum frequency of 0.017 Hz. Error bars were determined by taking the average of at least 100 measurements points (one measurement was performed per second).

3.4 *Evaluating of template-monomer binding by NMR analysis*

To further investigate the interactions between monomer and template, NMR titration experiments were performed. Instead of screening all monomers, solely interactions between methacrylic acid and caffeine were studied since the polymers prepared with this monomer had the highest affinity for

caffeine in the thermal analysis experiments. Appendix E, figure E.1 labels the protons present in caffeine and methacrylic acid that can be observed in the ^{1}H-NMR spectra.

Initial experiments were performed with methacrylic acid and caffeine at concentrations ranging from 0-100 mM. The peaks of the hydrogens labelled in Figure 8 did not shift significantly, indicating limited influence of the concentration on the chemical shifts. On the other hand, spectra of mixtures of MAA and caffeine in DMSO-d6 revealed a downfield shift (up to 0.04 ppm) of all the caffeine hydrogen atoms as the relative concentration of MAA increases (Figure 9). These shifts are similar to those observed in literature by Xu *et al*. [24].This suggests an electronic π-stacking interaction between both template and monomer and the observed deshielding effect is probably due to the electron-poor double bond of MAA attached to the electron-withdrawing carboxylic group. The NMR spectra of the peaks shifts of each caffeine marked hydrogen atom can be found in Appendix D, figure D.2.

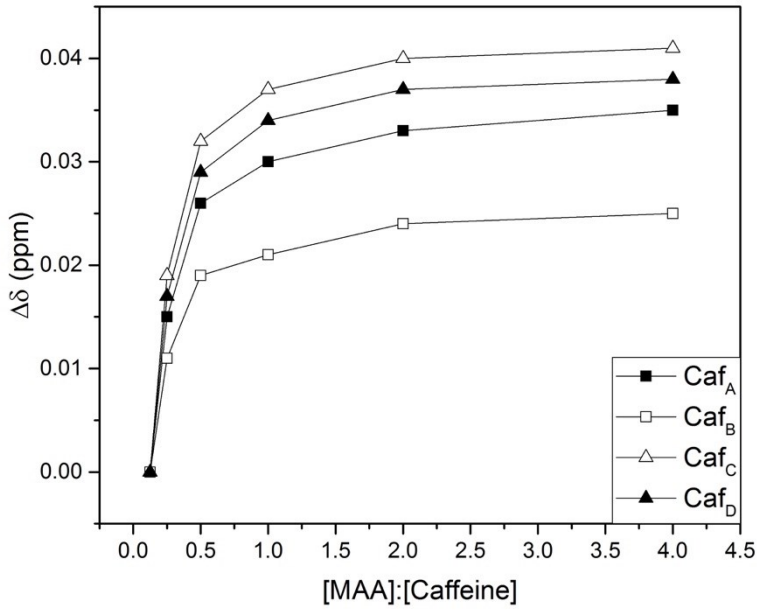

Figure 9. Differences in the chemical shifts of caffeine hydrogen atoms in function of the relative concentration of MAA. An internal reference, tetramethylsilane (TMS), was used in all experiments and the chemical shift of the caffeine peaks were related to that of the standard. The precision of the NMR experiments therefore corresponds to the precision of the machine (±0.01 ppm), which is well below the recorded shifts of 0.04 ppm.

4. Conclusions

MIPs for the detection of caffeine were synthesized with the monomers MAA, AA and HEMA. Batch rebinding experiments evaluated with spectroscopic methods determined that MIPs with AA as monomer exhibited the highest recognition capability (IF = 4.1) for caffeine. Subsequently, the prepared MIPs were integrated into SPEs by direct mixing of the particles with the screen-printing ink to obtain MIP-modified SPEs. However, AA is a soft material and was not compatible with the graphite based ink used in screen-printing which hindered incorporating of the particles in the ink. Therefore, it was decided to continue with MIPs with MAA as monomer (IF = 3.5), that demonstrated better miscibility and was able to go up to a particle vs ink ratio of 30 %. NMR analysis provided insight in the binding of MAA and caffeine, demonstrating shifts in the peaks upon titration that prove the complexation of the monomer and template.

MIP-modified SPEs (with MAA as monomer) were mounted into a home-made device and the thermal resistance was measured. First, PID settings were optimized and the influence of temperature on the noise on the signal was evaluated. It was shown that the noise on the signal was highly temperature dependent; at 90 °C a variation of 0.40 % on the signal was measured, contrary to 1 % at 37 °C. Subsequently, the sensitivity of the MIP-modified SPEs towards caffeine was determined by measuring the response to caffeine at temperatures 37, 50 and 85 °C. Using the HTM the LOD decreased from 40 nM at 37 °C to <1 nM at 85 °C, showing that the LOD can be fine-tuned by varying the temperature. TWTA was also performed at 85 °C, providing a similar LOD (~1 nM) at the optimal input frequency of 0.017 Hz. This is the first time HTM and TWTA measurements have been performed with MIPs at these elevated temperatures.

The sensor platform was proven to be specific since the corresponding NIP-SPEs showed no response to caffeine. In addition, selectivity was demonstrated by measuring the response of the MIP-modified SPEs towards similar molecules such as theophylline, theobromine and dopamine. Finally, as proof-of-application, MIP-modified SPEs were measured in complex matrices including coffee spiked samples and diluted tea samples. The spiking of coffee clearly led to a 21 % increase in thermal resistance. Furthermore, it was also possible to detect small amounts of caffeine, ~1 nM, in tea.

The developed sensor platform can measure caffeine concentrations at trace amounts, which enables the user to determine when drinking water samples are contaminated. The thermal set up is portable and can be brought on-site, is fast, and low-cost, making it perfectly suitable for environmental monitoring, even at remote locations. Molecular imprinting is versatile and by adapting the MIP, other micropollutants and potentially even large macromolecules, such as bacteria, can be targeted. This makes it a powerful tool for environmental analysis on-site, for which there is currently a high demand.

5. Acknowledgements

We would like to acknowledge the Royal Society of Chemistry for funding for research mobility of MP (visit to Universidade de São Paulo) and purchase of consumables with Research Fund RF18-2881 of MP. Furthermore, we would like to thank NC3Rs for PDRA position of RC. JG thanks Conselho Nacional de Desenvolvimento Científico e Tecnológico (CNPq) for the financial support (grant numbers: 306147/2016-5 and 400740/2014-1). We would like to thank Heitor Valarini (Universidade de São Paulo) and Amanpreet Kaur (Manchester Metropolitan University) for assistance with the experiments and stimulating discussions.

6. References

[1] K. Starke, Regulation of noradrenaline release by presynaptic receptor systems, Reviews of physiology, biochemistry and pharmacology 77 (1977) 1-124.
[2] M.W. Schwartz, S.C. Woods, D. Porte, Jr., R.J. Seeley, D.G. Baskin, Central nervous system control of food intake, Nature 404 (2000) 661-671.
[3] A.S. Jansen, X.V. Nguyen, V. Karpitskiy, T.C. Mettenleiter, A.D. Loewy, Central command neurons of the sympathetic nervous system: basis of the fight-or-flight response, Science (New York, N.Y.) 270 (1995) 644-646.
[4] S. Ferré, Caffeine and Substance Use Disorders, Journal of Caffeine Research 3 (2013) 57-58.
[5] Ignaz J. Buerge, Thomas Poiger, Markus D. Müller, H.-R. Buser, Caffeine, an Anthropogenic Marker for Wastewater Contamination of Surface Waters, (2003).
[6] W. Stumm, Chemical Processes in Lakes, Wiley1985.
[7] C.I. Kosma, D.A. Lambropoulou, T.A. Albanis, Occurrence and removal of PPCPs in municipal and hospital wastewaters in Greece, J Hazard Mater 179 (2010) 804-817.
[8] A.Y. Lin, Y.T. Tsai, Occurrence of pharmaceuticals in Taiwan's surface waters: impact of waste streams from hospitals and pharmaceutical production facilities, The Science of the total environment 407 (2009) 3793-3802.
[9] K.C. Machado, M.T. Grassi, C. Vidal, I.C. Pescara, W.F. Jardim, A.N. Fernandes, F.F. Sodre, F.V. Almeida, J.S. Santana, M.C. Canela, C.R.O. Nunes, K.M. Bichinho, F.J.R. Severo, A preliminary nationwide survey of the presence of emerging contaminants in drinking and source waters in Brazil, The Science of the total environment 572 (2016) 138-146.

[10] R. Tröger, P. Klöckner, L. Ahrens, K. Wiberg, Micropollutants in drinking water from source to tap - Method development and application of a multiresidue screening method, Science of The Total Environment 627 (2018) 1404-1432.
[11] B.L.M. H.-G. PÖTTERING, DIRECTIVE 2008/105/EC OF THE EUROPEAN PARLIAMENT AND OF THE COUNCIL of 16 December 2008 on environmental quality standards in the field of water policy, amending and subsequently repealing Council Directives 82/176/EEC, 83/513/EEC, 84/156/EEC, 84/491/EEC, 86/280/EEC and amending Directive 2000/60/EC of the European Parliament and of the Council, in: E.P.a.o.t. Council (Ed.) Directive 2008/105/ECOfficial Journal of the European Union, 2008, pp. 13.
[12] E.D.f. Umwelt, Revision der Gewässerschutzverordnung für bessere Wasserqualität, 2014.
[13] F. Gagne, C. Blaise, M. Fournier, P.D. Hansen, Effects of selected pharmaceutical products on phagocytic activity in Elliptio complanata mussels, Comparative biochemistry and physiology. Toxicology & pharmacology : CBP 143 (2006) 179-186.
[14] F. Gagné, E. Bérubé, M. Fournier, C. Blaise, Inflammatory properties of municipal effluents to Elliptio complanata mussels — lack of effects from anti-inflammatory drugs, Comparative Biochemistry and Physiology Part C: Toxicology & Pharmacology 141 (2005) 332-337.
[15] M. Capolupo, P. Valbonesi, A. Kiwan, S. Buratti, S. Franzellitti, E. Fabbri, Use of an integrated biomarker-based strategy to evaluate physiological stress responses induced by environmental concentrations of caffeine in the Mediterranean mussel Mytilus galloprovincialis, Science of The Total Environment 563-564 (2016) 538-548.
[16] Y. Zuo, H. Chen, Y. Deng, Simultaneous determination of catechins, caffeine and gallic acids in green, Oolong, black and pu-erh teas using HPLC with a photodiode array detector, Talanta 57 (2002) 307-316.
[17] P.R. Gardinali, X. Zhao, Trace determination of caffeine in surface water samples by liquid chromatography–atmospheric pressure chemical ionization–mass spectrometry (LC–APCI–MS), Environment International 28 (2002) 521-528.
[18] J. Zou, N. Li, Simple and environmental friendly procedure for the gas chromatographic–mass spectrometric determination of caffeine in beverages, Journal of Chromatography A 1136 (2006) 106-110.
[19] S.B. Hawthorne, D.J. Miller, J. Pawliszyn, C.L. Arthur, Solventless determination of caffeine in beverages using solid-phase microextraction with fused-silica fibers, Journal of Chromatography A 603 (1992) 185-191.
[20] T. Kobayashi, Y. Murawaki, P.S. Reddy, M. Abe, N. Fujii, Molecular imprinting of caffeine and its recognition assay by quartz-crystal microbalance, Analytica Chimica Acta 435 (2001) 141-149.
[21] J.J. Carvalho, M.G. Weller, U. Panne, R.J. Schneider, A highly sensitive caffeine immunoassay based on a monoclonal antibody, Analytical and Bioanalytical Chemistry 396 (2010) 2617-2628.
[22] J. Grandke, L. Oberleitner, U. Resch-Genger, L.-A. Garbe, R.J. Schneider, Quality assurance in immunoassay performance—comparison of different enzyme immunoassays for the determination of caffeine in consumer products, Analytical and Bioanalytical Chemistry 405 (2013) 1601-1611.
[23] W.S. R., Caffeine—A Drug with a Surprise, Angewandte Chemie International Edition 42 (2003) 604-605.
[24] W. Xu, T.-H. Kim, D. Zhai, J.C. Er, L. Zhang, A.A. Kale, B.K. Agrawalla, Y.-K. Cho, Y.-T. Chang, Make Caffeine Visible: a Fluorescent Caffeine “Traffic Light” Detector, Scientific Reports 3 (2013) 2255.
[25] A.K. Ghosh, C. Ghosh, A. Gupta, A Simple Approach To Detect Caffeine in Tea Beverages, Journal of Agricultural and Food Chemistry 61 (2013) 3814-3820.
[26] I. Baleviciute, V. Ratautaite, A. Ramanaviciene, Z. Balevicius, J. Broeders, D. Croux, M. McDonald, F. Vahidpour, R. Thoelen, W.D. Ceuninck, K. Haenen, M. Nesladek, A. Reza, A. Ramanavicius, Evaluation of theophylline imprinted polypyrrole film, Synthetic Metals 209 (2015) 206-211.
[27] V. Ratautaite, S.D. Janssens, K. Haenen, M. Nesládek, A. Ramanaviciene, I. Baleviciute, A. Ramanavicius, Molecularly Imprinted Polypyrrole Based Impedimentric Sensor for Theophylline Determination, Electrochimica Acta 130 (2014) 361-367.
[28] L. Ye, K. Haupt, Molecularly imprinted polymers as antibody and receptor mimics for assays, sensors and drug discovery, Analytical and Bioanalytical Chemistry 378 (2004) 1887-1897.

[29] K. Haupt, K. Mosbach, Molecularly Imprinted Polymers and Their Use in Biomimetic Sensors, Chemical Reviews 100 (2000) 2495-2504.
[30] V. Ratautaite, M. Nesladek, A. Ramanaviciene, I. Baleviciute, A. Ramanavicius, Evaluation of Histamine Imprinted Polypyrrole Deposited on Boron Doped Nanocrystalline Diamond, Electroanalysis 26 (2014) 2458-2464.
[31] J. Svenson, I.A. Nicholls, On the thermal and chemical stability of molecularly imprinted polymers, Analytica Chimica Acta 435 (2001) 19-24.
[32] R. Thoelen, R. Vansweevelt, J. Duchateau, F. Horemans, J. D'Haen, L. Lutsen, D. Vanderzande, M. Ameloot, M. vandeVen, T.J. Cleij, P. Wagner, A MIP-based impedimetric sensor for the detection of low-MW molecules, Biosensors and Bioelectronics 23 (2008) 913-918.
[33] Q. Zhu, C. Ma, H. Chen, Y. Wu, J. Huang, A molecular imprint-coated stirrer bar for selective extraction of caffeine, theobromine and theophylline, Microchimica Acta 181 (2014) 303-311.
[34] X. Liu, N. Sun, Q. Zhu, M. Wu, Y. Ye, H. Chen, Preparation, characterization and application of organic–inorganic hybrid caffeine imprinted monolith, 1304 (2013) 10-17.
[35] W.d.J.R. Santos, M. Santhiago, I.V.P. Yoshida, L.T. Kubota, Electrochemical sensor based on imprinted sol–gel and nanomaterial for determination of caffeine, 166-167 (2012) 739-745.
[36] I.-C. Chung, C.-C. Chang, H.-S. Chiu, S.-F. Jiang, M.-H. Lee, C.-L. Chung, B.-D. Liu, C.-Y. Huang, H.-Y. Lin, A Portable Electrochemical Sensor for Caffeine and (-)Epigallocatechin Gallate Based on Molecularly Imprinted Poly(ethylene-co-vinyl alcohol) Recognition Element, (2011).
[37] A. Ramanaviciene, A. Ramanavicius, A. Finkelsteinas, Basic Electrochemistry Meets Nanotechnology: Electrochemical Preparation of Artificial Receptors Based on Nanostructured Conducting Polymer, Polypyrrole, Journal of Chemical Education 83 (2006) 1212.
[38] V. Ratautaite, D. Plausinaitis, I. Baleviciute, L. Mikoliunaite, A. Ramanaviciene, A. Ramanavicius, Characterization of caffeine-imprinted polypyrrole by a quartz crystal microbalance and electrochemical impedance spectroscopy, Sensors and Actuators B: Chemical 212 (2015) 63-71.
[39] B. van Grinsven, K. Eersels, M. Peeters, P. Losada-Pérez, T. Vandenryt, T.J. Cleij, P. Wagner, The Heat-Transfer Method: A Versatile Low-Cost, Label-Free, Fast, and User-Friendly Readout Platform for Biosensor Applications, ACS Applied Materials & Interfaces 6 (2014) 13309-13318.
[40] B. van Grinsven, N. Vanden Bon, H. Strauven, L. Grieten, M. Murib, K.L. Jiménez Monroy, S.D. Janssens, K. Haenen, M.J. Schöning, V. Vermeeren, M. Ameloot, L. Michiels, R. Thoelen, W. De Ceuninck, P. Wagner, Heat-Transfer Resistance at Solid–Liquid Interfaces: A Tool for the Detection of Single-Nucleotide Polymorphisms in DNA, ACS Nano 6 (2012) 2712-2721.
[41] M. Peeters, P. Csipai, B. Geerets, A. Weustenraed, B. van Grinsven, R. Thoelen, J. Gruber, W. De Ceuninck, T.J. Cleij, F.J. Troost, P. Wagner, Heat-transfer-based detection of l-nicotine, histamine, and serotonin using molecularly imprinted polymers as biomimetic receptors, Analytical and Bioanalytical Chemistry 405 (2013) 6453-6460.
[42] P. Losada-Pérez, K.L. Jiménez-Monroy, B. van Grinsven, J. Leys, S.D. Janssens, M. Peeters, C. Glorieux, J. Thoen, K. Haenen, W. De Ceuninck, P. Wagner, Phase transitions in lipid vesicles detected by a complementary set of methods: heat-transfer measurements, adiabatic scanning calorimetry, and dissipation-mode quartz crystal microbalance, physica status solidi (a) 211 (2014) 1377-1388.
[43] M.M. Peeters, B. van Grinsven, C.W. Foster, T.J. Cleij, C.E. Banks, Introducing Thermal Wave Transport Analysis (TWTA): A Thermal Technique for Dopamine Detection by Screen-Printed Electrodes Functionalized with Molecularly Imprinted Polymer (MIP) Particles, Molecules (Basel, Switzerland) 21 (2016).
[44] J.-X. Dong, Q. Li, Z.-C. Tan, Z.-H. Zhang, Y. Liu, The standard molar enthalpy of formation, molar heat capacities, and thermal stability of anhydrous caffeine, The Journal of Chemical Thermodynamics 39 (2007) 108-114.
[45] F. Canfarotta, J. Czulak, K. Betlem, A. Sachdeva, K. Eersels, B. van Grinsven, T.J. Cleij, M. Peeters, A novel thermal detection method based on molecularly imprinted nanoparticles as recognition elements, Nanoscale 10 (2018) 2081-2089.
[46] S. Casadio, J.W. Lowdon, K. Betlem, J.T. Ueta, C.W. Foster, T.J. Cleij, B. van Grinsven, O.B. Sutcliffe, C.E. Banks, M. Peeters, Development of a novel flexible polymer-based biosensor platform for the thermal detection of noradrenaline in aqueous solutions, Chemical Engineering Journal 315 (2017) 459-468.

[47] K. Tyszczuk-Rotko, A. Szwagierek, Green Electrochemical Sensor for Caffeine Determination in Environmental Water Samples: The Bismuth Film Screen-Printed Carbon Electrode, Journal of The Electrochemical Society 164 (2017) B342-B348.
[48] N. Lezi, S. Economopoulos, M. Prodromidis, A. Economou, N. Tagmatarchis, Fabrication of a "Green" and Low–Cost Screen–Printed Graphene Sensor and Its Application to the Determination of Caffeine by Adsorptive Stripping Voltammetry International Journal of Electrochemical Science 12 (2017) 6054-6067.
[49] T. Alizadeh, M.R. Ganjali, M. Zare, P. Norouzi, Development of a voltammetric sensor based on a molecularly imprinted polymer (MIP) for caffeine measurement, Electrochimica Acta 55 (2010) 1568-1574.
[50] M. Zougagh, A. Ríos, M. Valcárcel, Automatic selective determination of caffeine in coffee and tea samples by using a supported liquid membrane-modified piezoelectric flow sensor with molecularly imprinted polymer, Analytica Chimica Acta 539 (2005) 117-124.

Appendix A – Thermogravimetric analysis

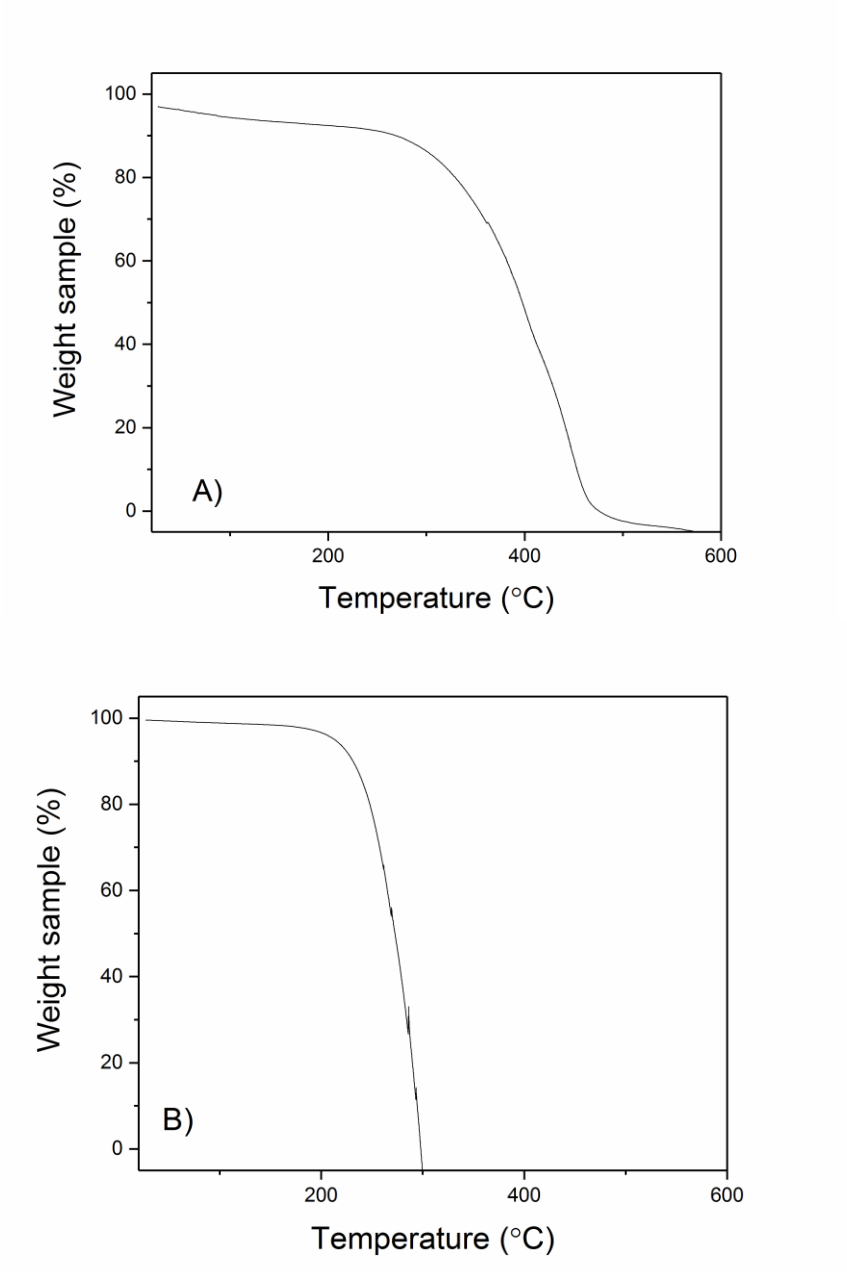

Figure A.1. Thermogravimetric analysis (TGA) was performed on the MIP (a) and caffeine (b). In both cases no noticeable weight loss was observed until ~200 °C, demonstrating the stability of both the polymer particles and template under measurement conditions (temperatures up to 85 °C).

Appendix B – NIP-SPEs (evaluation specificity)

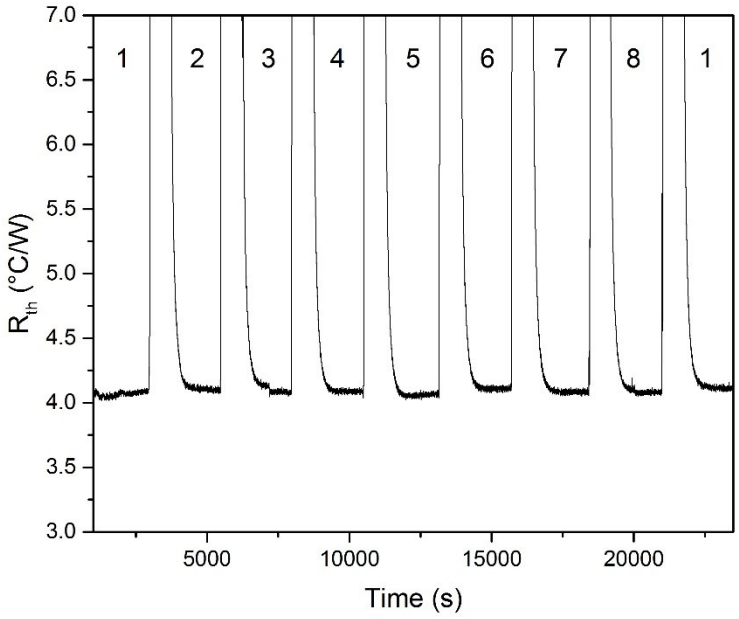

Figure B.1. demonstrates the thermal resistance in time at T = 85 °C when the NIP-SPEs were exposed to buffered caffeine solutions with increasing concentrations. The numbers correspond to additions of a pure PBS solution (1), and increasing concentration of caffeine (0, 2.5, 5, 10, 25, 50, 100, 250, 500 nM) indicated by numbers 2-8. The thermal resistance measured in buffered solution is similar to that of the MIP-modified SPE (~4.15 °C/W) but no significant increases were observed after addition of caffeine, indicating the the specificity of the sensor platform.

Appendix C – Reusability of MIP-based sensor platform

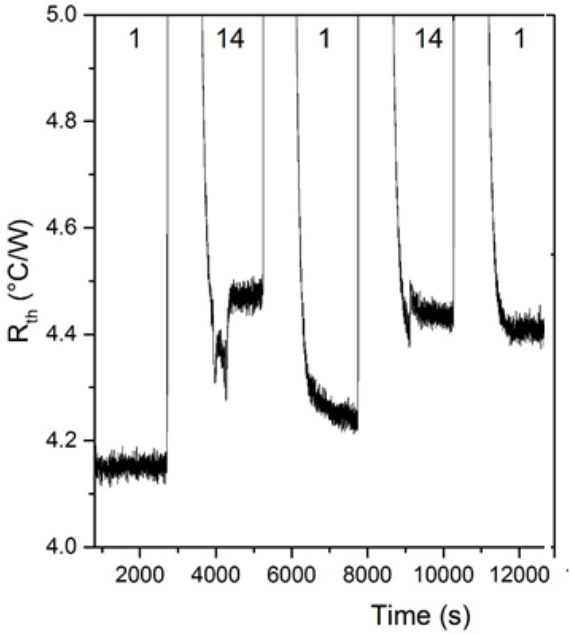

Figure C.1. The MIP-modified SPE (measured at T = 85 °C) with alternating injections of PBS (1) and 2.5 μM caffeine in PBS (14). It shows that washing with PBS is not sufficient to remove all caffeine from the MIP-modified SPE. The second exposure of the caffeine solution increased the thermal resistance to the same level but this time, washing with PBS did not have a significant impact on the signal.

Appendix D – MIP-SPEs: caffeine measured in the presence of theophylline

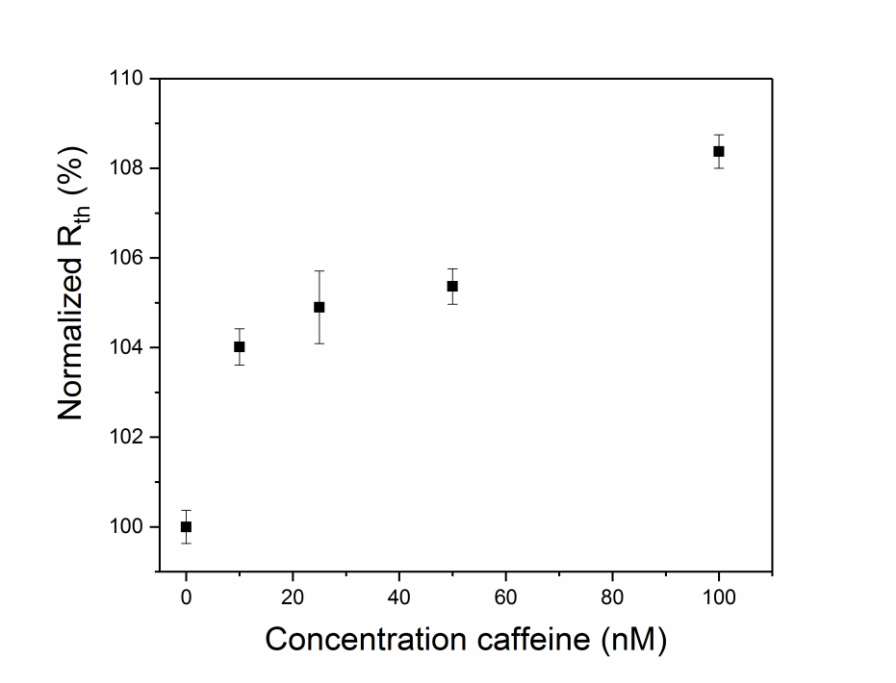

Figure D.1. The MIP-modified SPE (T = 85 °C) was measured in PBS containing an excess of theophylline (250 nM). The normalized R_{th} response at various concentration of caffeine (0-100 nM) was determined (with the error bars represeting the normalized standart deviaton on atleast 225 datapoints), with a maximum increase of 8.5% at the highest concentration. This is a factor of two lower compared to pure PBS, but the impact on the limit of detection (3-5 nM) is minimal. Therefore, and considering the similarity of theohpylline to caffeine, we are confident we can perform measurements in the presence of contaminants such as pharmaceuticals.

Appendix E – NMR titration experiments

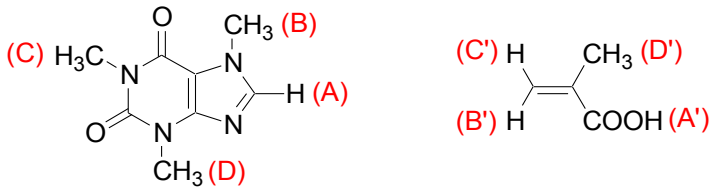

Figure E.1. Labelled protons of caffeine (left) and methacrylic acid (right) that can be observed in the ^{1}H-NMR spectra.

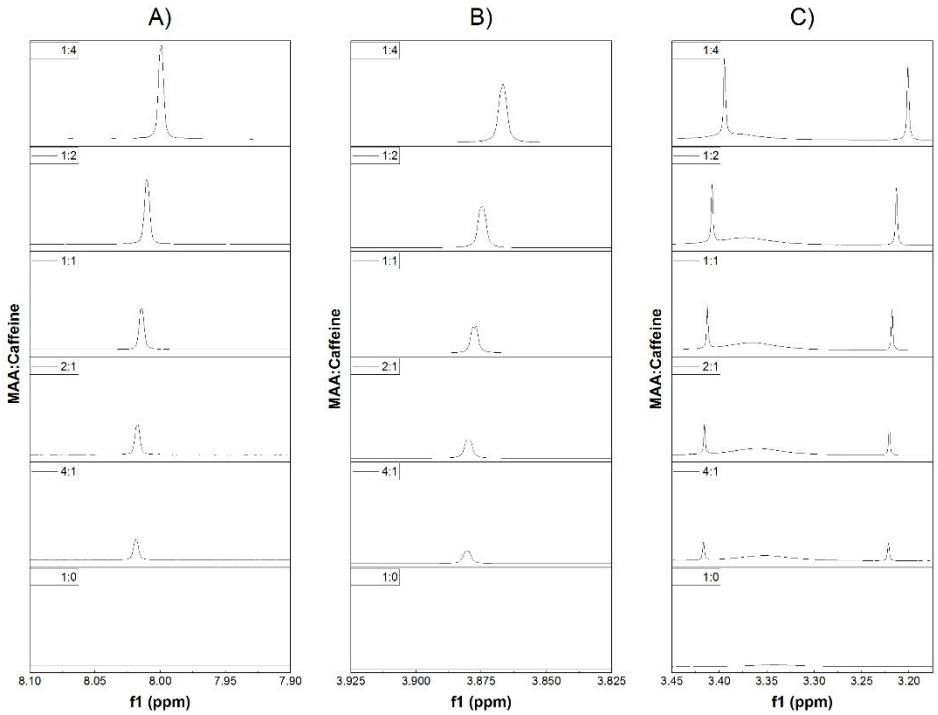

Figure E.2. Peak shifts with increasing caffeine concentrations. The molar ratio of MAA : caffeine is from bottom to top 1:4, 1:2, 1:1, 2:1, 4:1 and 1:0. The peak shift stack plot A corresponds to Caf_A, stack plot B with Caf_B and plot C shows the shift of Caf_C (left) and Caf_D (right).